Distributed Stochastic Security Constrained Unit Commitment for Coordinated Operation of Transmission and Distribution System

Aamir Nawaz, *Member, IEEE*, and Hongtao Wang, *Senior Member, IEEE*

***Abstract*—With the high penetration of renewable energies in modern power systems, deterministic coordination algorithms are facing two major problems: one is degradation in accuracy if fewer scenarios are utilized for uncertainty evaluation while second is the high computational time if a high number of scenarios are considered for better accuracy. In both cases, the efficiency of the algorithm is degraded. To solve these problems in coupled transmission system and distribution systems (TSDS), probabilistic coordination algorithms are adopted to solve with less effort. In this paper, a TSDS probabilistic coordination model is proposed to solve the coordinated security-constrained unit commitment problem. A mean and standard deviation matching based probabilistic analytical target cascading algorithm has been utilized for evaluation of TSDS coordination problem. Instead of solving each scenario as a separate problem, the proposed algorithm considers a single coordination problem with probabilistic characteristics as shared variables and hence, achieves fast convergence. Different case studies are performed to prove the efficacy of the proposed algorithm. Results verify that the proposed algorithm reduces computational time and resources for large-scale systems.**

***Index Terms*—Distribution system, mean, probabilistic analytical, standard deviation, target Cascading, transmission system.**

NOMENCLATURE

A. Parameters

$i, m, t, h,$ n, j, k	Index of DSOs, buses, hours, up/down unit's hours, generators, inner loop and outer loop.
$\rho, \eta, \alpha, \beta$	Multipliers for generalized PATC.
$\rho^k_{\mathrm{DSO}i}, \eta^k_{\mathrm{DSO}i},$ $\alpha^k_{\mathrm{DSO}i}, \beta^k_{\mathrm{DSO}i}$	Multipliers for augmented Lagrange penalty function.
w_μ, w_σ	Multipliers for generalized PATC.
$w^{\mathrm{DSO}i,k}_\mu,$ $w^{\mathrm{DSO}i,k}_\sigma$	Multipliers for quadratic penalty functions of the mean and the standard deviation for ith DSO.
$\gamma_1, \gamma_2, \gamma_3, \gamma_4$	Pre-defined factors.
$\varepsilon_1, \varepsilon_2, \varepsilon_3$	Thresholds for evaluation of various errors.
up_n, dn_n	Starting hour for unit up and unit down time.

B. Functions and Variables

c_{nt}	Cost function.
$P^0_{nt}, P^s_{nt},$ I^0_{nt}, I^s_{nt}	Base and scenario case output power and on/off index of nth generator at tth hour.
p_s	Probability of cost contribution for each scenario.
ΔP^s_{nt}	Change in base and scenario case power generation.
$SUD_{nt},$ $MUT_n,$ MDT_n	Shutdown/start-up costs, uptime, and downtime for nth generator.
$P^0_{n(t+1)}, P^0_{wt},$ $PL^0_{lt}, D^0_t,$ $P^s_{nt}, P^s_{wt},$ PL^s_{lt}, D^s_t	Active generation of nth generator for $(t+1)$th hour, wth wind farm output, lth line losses and demand at tth hour for base case and scenario case.
$Q^0_{nt}, Q^0_{wt},$ $QB^0, QD^0_t,$ $Q^s_{nt}, Q^s_{wt},$ QB^s, QD^s_t	Reactive generation of nth generator for tth hour, wth wind farm output, lth line losses and demand at tth hour for base case and scenario case.
$\delta^0_{mt}, \delta^{\min}_m,$ $\delta^{\max}_m, V^0_{mt},$ $V^{\min}_m, V^{\max}_m$	Angle and voltage at mth bus, their minimum and maximum limits.
$P^{\min}_n, P^{\max}_n$	Minimum and maximum generation limit of units.
$R^{0,up}_n, R^{0,dn}_n,$ $R^{s,up}_n, R^{s,dn}_n$	Up and down reserves for base and scenario case.
$P^0_{f,wt}, P^s_{f,wt}$	Forecasted wind power generation for base and scenario case.
LSF	Line shift factors.
$T^{\mathrm{DSO}i},$ $R^{\mathrm{DSO}i}$	Targets from TSO to ith DSO and responses vice versa.
$f^{\mathrm{TSO}},$ x^{TSO}	Deterministic and non-separable TSO objective and it's variable.
$h^{\mathrm{TSO}},$ g^{TSO}	Deterministic equality and inequality constraints for TSO.
$f^{\mathrm{DSO}i},$ $x^{\mathrm{DSO}i}$	Deterministic non-separable objective of ith DSO and it's variable.
$h^{\mathrm{DSO}i},$ $g^{\mathrm{DSO}i}$	Deterministic equality and inequality constraints for ith DSO.
$f^{\mathrm{TSO}}_y,$ $f^{\mathrm{DSO}i}_y,$	Deterministic separable TSO objective, ith DSO objective and shared variable
y	Generalized penalty function.

Manuscript received May 27, 2020; revised August 1, 2020; accepted September 9, 2020. Date of online publication October 6, 2020; date of current version March 16, 2020. This work was supported by the National Key R&D Program of China (2016YFB0900100).

A. Nawaz and H. T. Wang (corresponding author, e-mail: whtwhm@sdu.edu.cn; ORCID: https://orcid.org/0000-0002-5522-455X) are with the Key Laboratory of Power System Intelligent Dispatch and Control of Ministry of Education, Shandong University, Jinan 250000, China.

DOI: 10.17775/CSEEJPES.2020.02150

$h_y^{\mathrm{TSO}}, g_y^{\mathrm{TSO}}, h_y^{\mathrm{DSO}i}, g_y^{\mathrm{DSO}i}$	Deterministic equality and inequality constraints for TSO.
f^v, X^v, T^v, R^v	Probabilistic coordinated objective function, its random variable, targets and responses.
g_m^v, h_m^v, ω_m	Random values based on inequality and equality constraints and conditional probability value.
$\mu_{T^v}, \mu_{R^v}, \sigma_{T^v}, \sigma_{R^v}$	Mean and standard deviation of random value target and responses respectively.
$f_Y^{v,\mathrm{TSO}}, X^{v,\mathrm{TSO}}, Y$	Probabilistic coordinated TSO objective, its random variable and shared variable.
$T^{v,\mathrm{DSO}i}, R^{v,\mathrm{DSO}i}$	Random value targets from TSO to ith DSO and random value responses vice versa.
$g_Y^{v,\mathrm{TSO}}, h_Y^{v,\mathrm{TSO}}$	Random characteristics based on inequality and equality constraints for TSO.
$f_Y^{v,\mathrm{DSO}i}, X^{v,\mathrm{DSO}i}, Y$	Probabilistic coordinated objective of ith DSO, its random and shared variable.
$g_s^{v,\mathrm{DSO}i}, h_s^{v,\mathrm{DSO}i}$	Random characteristics based on inequality and equality constraints for ith DSO.
$P^{v,\mathrm{TSO}}, P^{v,\mathrm{DSO}i}$	Random power generation (including the base case and scenarios) in TSO and DSOs due to wind farms and random load.
$\mu_{PG^{\mathrm{DSO}i}}, \mu_{PD^{\mathrm{DSO}i}}, \sigma_{PG^{\mathrm{DSO}i}}, \sigma_{PD^{\mathrm{DSO}i}}$	Mean and standard deviation of targets and responses.
$Sysk_{\mathrm{cost}}^k, TS_{\mathrm{cost}}^k, DS_{\mathrm{cost}}^{i,k}$	The overall system, TS and DS cost.

I. Introduction

In the modern era of power systems, different countries are following three coordination conceptual frameworks for the transmission system operator (TSO) and distribution system operator (DSO), which are stated as Total TSO, Hybrid TSO and Total DSO [1]. In these frameworks, TSO and DSO are assigned individual or mutual controlled distributed energy resources (DERs) through aggregators. As the TSO DSO framework is emerging, the algorithms should emerge to deal with advanced coordination problems.

High penetration of renewable energies in power systems have opened a new era of research in the coordination of transmission and distribution systems. The European Network of Transmission System Operators for Electricity (ENTSO-E) has discussed the benefits of optimally coordinated access of resources within TSO and DSOs [2]. This can help system operators in handling problems [3], such as system balancing and congestion management, etc. It is reported in California that a high penetration of renewable energies in distribution systems [4], will create significant difficulties for transmission system operations, which are difficult to manage via the current separate management method [5]. An outage event caused approximately 2.7 million customers to be without power on a hot day, which was indicated as a lack of coordination between the transmission system and the distribution systems (TSDS) in the report of the Federal Energy Regulatory Commission (FERC) and North American Electric Reliability Corporation (NERC) [6]. This has provided motivation to research new coordination methods for solving probabilistic coordination problems under the impact of high scale renewable energy.

Nowadays, wind farms are considered as favorable sources to serve loads. Due to the large-scale integration of wind farms, their contribution has been dramatically increased in power system economics [7]. Still, critical system management issues are arising due to the presence of high penetration of wind farms, which is due to the uncertain behavior of wind. Power system operators are required to predict and mitigate system violations due to wind uncertainty and provide continuous power to customers. Previously, researchers have introduced three different approaches, such as chance-constrained optimization [8], robust optimization [9], and stochastic optimization [10] to solve the uncertainty problems in power systems due to renewable energies. Moreover, distributed TSO and DSO coordination has been previously investigated in large-scale power systems for scheduling problems such as optimal power flow (OPF) [11], [12], risk-aware OPF [13] and security-constrained unit commitment (SCUC) [14], [15]. However, due to the high penetration of renewable energies in power systems, researchers are required to investigate stochastic security-constrained unit commitment while providing stochastic coordination between TSO and DSO [16], [17].

This paper deals with the probabilistic coordination based stochastic unit commitment problem of TS and DS. While discussing the stochastic unit commitment, reference [18] has solved this problem using separate modules for unit commitment (UC), optimal power flow (OPF), and the bridge between UC and OPF modules. Previous studies have carried out multi-area stochastic coordination with large scale integration of wind farms [19], since each scenario is considered as a separate coordination problem. Therefore, for s scenarios, s coordination problems are solved. This means that the size of the probabilistic problem will increase with the number of scenarios. Yet, it is essential to select an optimal and comparatively large number of scenarios for precisely representing the behavior of wind farms and other uncertainties in power systems, as the accuracy of results will be decreased with a lesser number of scenarios [19]. Thus, stochastic coordination algorithms need to be investigated which consider a large number of optimally selected scenarios and also have fast convergence. Furthermore, such algorithms should consider base and scenario cases as a single stochastic coordination problem to reduce the complexity of the algorithm [20], [21].

In this paper, a stochastic coordination model is proposed to involve renewable uncertainties of sharing variables. The main contributions of this paper involve:

- A probabilistic TSDS coordination model based on probabilistic analytical target cascading (PATC) is proposed to solve a stochastically coordinated security-constrained unit commitment problem.
- To reduce computational time, the mean and standard deviation of shared variables is utilized instead of evaluating the coordination problem for each scenario [19].

This paper is divided into further sections as follows. Section II describes the hierarchical stochastic TSDS coordination strategy, Section III provides proposed methods for solving the stochastic coordination problem, Section IV presents results and discussion, and Section V provides the conclusion and future directions.

II. Description of Hierarchical Stochastic TSDS Coordination Based Stochastic Unit Commitment Framework

One of the most important factors in coordination algorithms is to share as little information as possible to keep up with the privacy rules of different areas. Two moments/probabilistic characteristic matching methods for probabilistic coordination have the advantage of sharing less information with other systems and thus, can assure the privacy of system information. Additionally, system resource utilization can be reduced, when mean and standard deviations are utilized as shared variables.

A. Generalized Stochastic Security Constrained Unit Commitment Problem Model

SCUC is referred to as one of the most important decision-making processes for the economically scheduling of energy resources while satisfying system demands and security constraints [22]. The objective function of generalized stochastic SCUC is shown as:

$$\min \sum_t \sum_n \left\{ c_{nt}\left(P_{nt}^0\right) I_{nt}^0 + SUD_{nt} \right\} + \sum_{s=1}^{\mathrm{NS}} p_s \left\{ \sum_t \sum_n c_{nt}\left(\Delta P_{nt}^s\right) I_{nt}^s \right\} \tag{1}$$

Base case constraints:

$$\text{s.t. } \sum_n P_{nt}^0 + \sum_w P_{wt}^0 + PB^0 = D_t^0 \tag{2}$$

$$P_n^{\min} I_{nt} \leqslant P_{nt}^0 \leqslant P_n^{\max} I_{nt} \tag{3}$$

$$\begin{cases} P_{n(t+1)}^0 - P_{nt}^0 \leqslant R_n^{0,up} I_{nt} \\ P_{nt}^0 - P_{n(t+1)}^0 \leqslant R_n^{0,dn} I_{nt} \end{cases} \tag{4}$$

$$0 \leqslant P_{wt}^0 \leqslant P_{f,wt}^0 \tag{5}$$

$$\begin{cases} I_{nt}^0 = 1, \text{ if } \sum\limits_{h=t-up_n}^{t-1} I_{nt}^0 < MUT_n \\ I_{nt}^0 = 1, \text{ if } \sum\limits_{h=t-dn_n}^{t-1} \left(1 - I_{nt}^0\right) < MDT_n \end{cases} \tag{6}$$

Scenario case constraints:

$$\text{s.t. } \sum_n P_{nt}^s + \sum_w P_{wt}^s + PB^s = D_t^s \tag{7}$$

$$P_n^{s,\min} I_{nt} \leqslant P_{nt}^s \leqslant P_n^{s,\max} I_{nt} \tag{8}$$

$$\begin{cases} P_{nt}^s - P_{nt}^0 \leqslant R_n^{s,up} I_{nt} \\ P_{nt}^0 - P_{nt}^s \leqslant R_n^{s,dn} I_{nt} \end{cases} \tag{9}$$

$$0 \leqslant P_{wt}^s \leqslant P_{f,wt}^s \tag{10}$$

$$\begin{cases} I_{nt}^s = 1, \text{ if } \sum\limits_{h=t-up_n}^{t-1} I_{nt}^s < MUT_n \\ I_{nt}^s = 1, \text{ if } \sum\limits_{h=t-dn_n}^{t-1} \left(1 - I_{nt}^s\right) < MDT_n \end{cases} \tag{11}$$

Here, $PB^0 = PG^0, PB^s = PG^s$ for TS and $PB^0 = -PD^0, PB^s = -PD^s$ for DS. Then, this formulation can be utilized by TSO or DSO while keeping in view the relevant variables of PB^0 and PB^s.

For security-constrained unit commitment evaluation, shift factors are utilized as Global shift factors [23]. Equation (12) and (13) are network security constraints

$$\sum LSF \left(\sum_n P_{nt}^s + \sum_w P_{wt}^s - D_t^s + PB^s \right) \geqslant -PL_l^{\max} \tag{12}$$

$$\sum LSF \left(\sum_n P_{nt}^s + \sum_w P_{wt}^s - D_t^s + PB^s \right) \leqslant PL_l^{\max} \tag{13}$$

As resistance is not negligible in the distribution system, therefore, the line losses should be considered in the DS. Hence, equation (2)–(3), (7)–(8), (12) and (13) are rewritten for DS as follows:

$$\begin{cases} \sum\limits_n P_{nt}^0 + \sum\limits_w P_{wt}^0 - \sum\limits_l PL_{lt}^0 + PB^0 = D_t^0 \\ \sum\limits_n Q_{nt}^0 + \sum\limits_w Q_{wt}^0 + QB^0 = QD_t^0 \end{cases} \tag{2A}$$

$$\begin{cases} P_n^{\min} I_{nt} \leqslant P_{nt}^0 \leqslant P_n^{\max} I_{nt} \\ Q_n^{\min} I_{nt} \leqslant Q_{nt}^0 \leqslant Q_n^{\max} I_{nt} \\ \delta_m^{\min} \leqslant \delta_{mt}^0 \leqslant \delta_m^{\max} \\ V_m^{\min} \leqslant V_{mt}^0 \leqslant V_m^{\max} \end{cases} \tag{3A}$$

$$\begin{cases} \sum\limits_n P_{nt}^s + \sum\limits_w P_{wt}^s - \sum\limits_l PL_{lt}^s + PB^s = D_t^s \\ \sum\limits_n Q_{nt}^s + \sum\limits_w Q_{wt}^s + QB^s = QD_t^s \end{cases} \tag{7A}$$

$$\begin{cases} P_n^{s,\min} I_{nt} \leqslant P_{nt}^s \leqslant P_n^{s,\max} I_{nt} \\ Q_n^{s,\min} I_{nt} \leqslant Q_{nt}^s \leqslant Q_n^{s,\max} I_{nt} \\ \delta_m^{\min} \leqslant \delta_{mt}^s \leqslant \delta_m^{\max} \\ V_m^{\min} \leqslant V_{mt}^s \leqslant V_m^{\max} \end{cases} \tag{8A}$$

$$\sum LSF \left(\sum_n P_{nt}^s + \sum_w P_{wt}^s - \sum_l PL_{lt}^0 - D_t^s + PB^s \right) \geqslant -PL_l^{\max} \tag{12A}$$

$$\sum LSF \left(\sum_n P_{nt}^s + \sum_w P_{wt}^s - \sum_l PL_{lt}^0 - D_t^s + PB^s \right) \leqslant PL_l^{\max} \tag{13A}$$

B. Generalized Formulation for Probabilistic Hierarchical Coordination

This section will introduce the coordination strategy of probabilistic hierarchical coordination for TS and DS. The proposed coordination strategy has been divided into inter-TSDS coordination and an intra-transmission system to the transmission system (TSTS) and distribution system to distribution system (DSDS) coordination using some linkage variables as shown in equation (14). This coordination strategy is illustrated in Fig. 1. It depicts the inter-TSDS coordination and strategy of sharing boundary information between TS and DS. It should be noted that the boundary information will be the stochastic variables. In intra-TSTS and DSDS

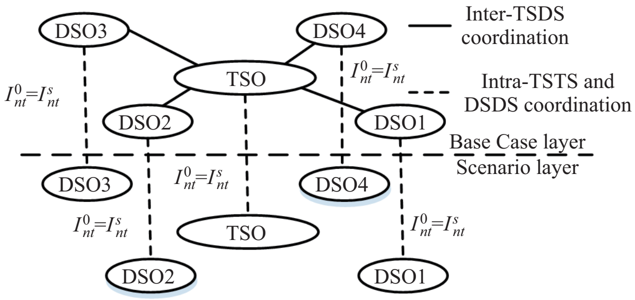

Fig. 1. Base case and scenario layer architecture for inter and intra TSO DSO probabilistic coordination.

coordination, base case and scenario layers are interconnected with the constraint given in (14).

$$I_{nt}^{0} = I_{nt}^{s} \tag{14}$$

To speed up the proposed solution, the individual area's uncertainty is dealt with in the scenario layer, and the relationship between the base case and scenarios are formulated. In inter-TSDS coordination, the main problem (1) is decomposed into the base case problem and multiple tractable and separable stochastic security constraint unit commitment (SSCUC) problems. Yet, for information sharing, boundary bus power flow should be modeled properly. It should be noted that in TS, DS is modeled as a pseudo load connected at boundary bus while in each DS, TS is modeled as a pseudo source at boundary bus [14].

1) Deterministic ATC Formulation for TSDS Coordination

TSO and DSO formulation can be expressed as given in equation (15) and (16). Still, these formulations show no coordination between TSO and DSO for optimal system operation.

$$\begin{aligned} \min\ & f^{\mathrm{TSO}}\left(x^{\mathrm{TSO}}\right) \\ \text{s.t. } & h^{\mathrm{TSO}}\left(x^{\mathrm{TSO}}\right) \leqslant 0 \\ & g^{\mathrm{TSO}}\left(x^{\mathrm{TSO}}\right) = 0 \end{aligned} \tag{15}$$

$$\begin{aligned} \min\ & f^{\mathrm{DSO}i}\left(x^{\mathrm{DSO}i}\right) \\ \text{s.t. } & h^{\mathrm{DSO}i}\left(x^{\mathrm{DSO}i}\right) \leqslant 0 \\ & g^{\mathrm{DSO}i}\left(x^{\mathrm{DSO}i}\right) = 0 \end{aligned} \tag{16}$$

For a deterministic ATC coordination algorithm, a separable formulation for TSO and DSO is required, which is given in (17) and (18):

$$\begin{aligned} \min\ & f_{y}^{\mathrm{TSO}}\left(x^{\mathrm{TSO}}, y\right) + \sum_{i=1}^{I} \pi\left(T^{\mathrm{DSO}i} - R^{\mathrm{DSO}i}\right) \\ \text{s.t. } & h^{\mathrm{TSO}}\left(x^{\mathrm{TSO}}, y\right) \leqslant 0 \\ & g^{\mathrm{TSO}}\left(x^{\mathrm{TSO}}, y\right) = 0 \end{aligned} \tag{17}$$

$$\begin{aligned} \min\ & f_{y}^{\mathrm{DSO}i}\left(x^{\mathrm{DSO}i}, y\right) + \pi(R^{\mathrm{DSO}i} - T^{\mathrm{DSO}i}) \\ \text{s.t. } & h_{y}^{\mathrm{DSO}i}\left(x^{\mathrm{DSO}i}, y\right) \leqslant 0 \\ & g_{y}^{\mathrm{DSO}i}\left(x^{\mathrm{DSO}i}, y\right) = 0 \end{aligned} \tag{18}$$

Here, $T^{\mathrm{DSO}i}$ represents the targets from TSO to ith DSO, and $R^{\mathrm{DSO}i}$ represents the responses from ith DSO to TSO, and π represents the penalty function, which is selected for optimal probabilistic coordination. The basic ATC algorithm has different penalty functions, such as linear penalty, quadratic penalty, Lagrange penalty, and exponential penalty, etc.

2) Probabilistic ATC Formulation for TSDS Coordination

For probabilistic coordination, shared variables are considered as random variables. To share information, the probability density function (PDF) of the shared variables is considered instead of a single deterministic value. Nevertheless, sharing PDF as shared variables (targets and responses) between TS and DS is impractical and inefficient. Therefore, targets and responses should represent the stochastic characteristics of their PDFs. For example, instead of providing stochastic data of 10,000 or more samples on the boundary of the area, it is efficient to share moments/characteristics of probabilistic distribution, such as mean, standard deviation, variance, skewness, and kurtosis. Although, for better results and less complexity, this paper has considered mean and standard deviation as targets and responses. Equation (19) shows the generalized formulation for PATC problems.

$$\begin{aligned} \min\ & f_{Y}^{v}\left(X^{v}, Y\right) + \pi\left(\|T^{v} - R^{v}\|\right) \\ \text{s.t. } & P_{r}\left[g_{Y,m}^{v}\left(X^{v}, Y\right) \leqslant 0\right] \geqslant \omega_{m}, \\ & m = 1, 2, 3, \ldots, M \\ & P_{r}\left[h_{Y,m'}^{v}\left(X^{v}, Y\right) = 0\right] \geqslant \omega_{m'}, \\ & m' = 1, 2, 3, \ldots, M' \end{aligned} \tag{19}$$

Here, X is considered a normally distributed random variable where $X^{v} = [\mu_{X}, \sigma_{X}]$, ω_{m} and $\omega_{m'}$ are thresholds for inequality and equality constraint, m is the number of inequality constraints and m' is the number of equality constraints. Additionally, equation (19) can be utilized to convert deterministic ATC formulations of TSO and DSO (in (17) and (18) respectively) to PATC formulations as shown in (20) and (21)

$$\begin{aligned} \min\ & f_{Y}^{v,\mathrm{TSO}}\left(X^{v,\mathrm{TSO}}, Y\right) + \sum_{i=1}^{I} \pi\left(T^{v,\mathrm{DSO}i} - R^{v,\mathrm{DSO}i}\right) \\ \text{s.t. } & P_{r}\left[g_{m}^{v,\mathrm{TSO}}\left(X^{v,\mathrm{TSO}}, Y\right) \leqslant 0\right] \geqslant \omega_{m}, \\ & m = 1, 2, 3, \ldots, M \\ & P_{r}\left[h_{m'}^{v,\mathrm{TSO}}\left(X^{v,\mathrm{TSO}}, Y\right) = 0\right] \geqslant \omega_{m'}, \\ & m' = 1, 2, 3, \ldots, M' \end{aligned} \tag{20}$$

$$\begin{aligned} \min\ & f_{Y}^{v,\mathrm{DSO}i}\left(X^{v,\mathrm{DSO}i}, Y\right) + \sum_{i=1}^{I} \pi\left(R^{v,\mathrm{DSO}i} - T^{v,\mathrm{DSO}i}\right) \\ \text{s.t. } & P_{r}\left[g_{m}^{v,\mathrm{DSO}i}\left(X^{v,\mathrm{DSO}i}, Y\right) \leqslant 0\right] \geqslant \omega_{m}, \\ & m = 1, 2, 3, \ldots, M \\ & P_{r}\left[h_{m'}^{v,\mathrm{DSO}i}\left(X^{v,\mathrm{DSO}i}, Y\right) \leqslant 0\right] \geqslant \omega_{m'}, \\ & m' = 1, 2, 3, \ldots, M' \end{aligned} \tag{21}$$

Hence, equations (20) and (21) show generalized objective functions for TSO and DSO probabilistic coordination.

III. Proposed Methods for Solving the Stochastically Coordinated TSDS Based SSCUC Problem

To solve the SSCUC problem of stochastically coordinated TSDS, two different methods of probabilistic coordination based on mean and standard deviation are proposed. The two methods differ based on the use of different penalty functions and are described in detail in the following sections. The random targets and responses in the generalized formula are converted to the mean and standard deviation of the corresponding targets and responses. Fig. 2 shows the basic architecture of the TSO and DSO probabilistic coordination framework with the mean and standard deviation as the shared variables.

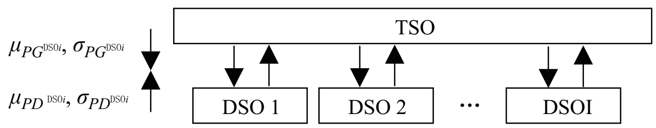

Fig. 2. Stochastic coordination scheme between TSO and DSO.

In TS, line resistances as compared to line reactances are negligible, so the ACOPF model can be relaxed to a DCOPF model. Hence, OPF in TS is referred to as DCOPF. In this way, voltage magnitude at every node of transmission is assumed as 1.0 p.u, and only active power is considered. While for DS, ACOPF is utilized as the ratio of resistance to line reactance, which is large. Accordingly, distribution terminal voltages can vary between 0.95 and 1.05 p.u. Furthermore, probabilistic OPF is considered between TS and DS, thus, the distribution system shares mean and standard deviation of active power information while reactive power sharing information is not included. To model reactive power mismatch at the border between TS and DSs, the voltage at the TS boundary terminal is considered one while the distribution boundary terminal voltages can vary between 0.95 and 1.05 p.u. However, reactive power mismatch is reduced by bringing the boundary terminal voltage to approximately 1 p.u. This paper does not consider the voltage stability problem.

A. Proposed Method I: Formulation of Mean and Standard Deviation Based Stochastic Coordination for Solving SSCUC with Lagrange Penalty

Proposed method I (PM-I) utilizes the Lagrange penalty function for evaluation of the SSCUC problem. The generalized equation is presented in (19) and can be rewritten as:

$$\begin{aligned}\min\ & f_Y^v\left(X^v,Y\right)+\rho\left(\mu_{T^v}-\mu_{R^v}\right)+\left\|\eta\circ\left(\mu_{T^v}-\mu_{R^v}\right)\right\|^2+\\ & \alpha\left(\sigma_{T^v}-\sigma_{R^v}\right)+\left\|\beta\circ\left(\sigma_{T^v}-\sigma_{R^v}\right)\right\|^2\\ \text{s.t. } & P_r\left[g_{Y,m}^v\left(X^v,Y\right)\leqslant 0\right]\geqslant\omega_m,\\ & m=1,2,3,\ldots,M\\ & P_r\left[h_{Y,m'}^v\left(X^v,Y\right)=0\right]\geqslant\omega_{m'},\\ & m'=1,2,3,\ldots,M'\end{aligned}\tag{22}$$

In this formulation, the mean and standard deviation are utilized for more accuracy in utilizing the Lagrange penalty function. In addition, the mean and standard deviation of boundary random variables of areas are utilized in the penalty function of each area in an appropriate way to separate the functions. Apart from the penalty function in the separable objective function, the area's non-separable objective function is evaluated for all scenarios. Then, it is utilized as a mean and standard deviation of the non-separable function in the separable objective function. It should be noted here that the cost affiliated with $PD^{v,\mathrm{DSO}i}$ is satisfied by $PG^{v,\mathrm{DSO}i}$ of the other area. Consequently, this term is not included in the objective function formulation. Additionally, in equations (20) and (21), T^v and R^v are replaced by $T^{v,\mathrm{DSO}i}$ and $T^{v,\mathrm{DSO}i}$ to acquire the TSO and DSO formulation. Thereby in equation (22), $\mu_{T^v}=\mu_{PG^{\mathrm{DSO}i}}$, $\mu_{R^v}=\mu_{PD^{\mathrm{DSO}i}}$, $\mu_{T^v}=\mu_{PG^{\mathrm{DSO}i}}$, $\mu_{R^v}=\mu_{PD^{\mathrm{DSO}i}}$ substitutions can be made for the TSO and DSO formulations in (23) and (29).

1) TSO Formulation

$$\min\left\{\begin{array}{l}f_n^{v,\mathrm{TSO}}\left(P^{v,\mathrm{TSO}},\mu_{PD^{\mathrm{DSO}i}},\sigma_{PD^{\mathrm{DSO}i}}\right)+\\ \sum\limits_{i=1}^{I}\left\{\begin{array}{l}\rho_{\mathrm{DSO}i}^k(\mu_{PD^{\mathrm{DSO}i}}-\mu_{PG^{\mathrm{DSO}i}})+\\ \left\|\eta_{\mathrm{DSO}i}^k\circ(\mu_{PD^{\mathrm{DSO}i}}-\mu_{PG^{\mathrm{DSO}i}})\right\|^2+\\ \alpha_{\mathrm{DSO}i}^k(\sigma_{PD^{\mathrm{DSO}i}}-\sigma_{PG^{\mathrm{DSO}i}})+\\ \left\|\beta_{\mathrm{DSO}i}^k\circ(\sigma_{PD^{\mathrm{DSO}i}}-\sigma_{PG^{\mathrm{DSO}i}})\right\|^2\end{array}\right\}\end{array}\right\}\tag{23}$$

where

$$\begin{aligned}&f_n^{v,\mathrm{TSO}}\left(P^{v,\mathrm{TSO}},\mu_{PD^{\mathrm{DSO}i}},\sigma_{PD^{\mathrm{DSO}i}}\right)=\\ &\min\sum_t\sum_n\left\{\begin{array}{l}\left\{c_{nt}\left(P_{nt}^{0,\mathrm{TSO}}\right)I_{nt}^{0,\mathrm{TSO}}+SUD_{nt}\right\}+\\ \sum\limits_{s=1}^{\mathrm{NS}}p_s\left\{\sum\limits_t\sum\limits_n c_{nt}\left(\Delta P_{nt}^{s,\mathrm{TSO}}\right)I_{nt}^{s,\mathrm{TSO}}\right\}\end{array}\right\}\end{aligned}\tag{24}$$

Subject to:
Constraints are given in (2)–(14)

$$\Delta P_{nt}^{s,\mathrm{TSO}}=P_{nt}^{s,\mathrm{TSO}}-P_{nt}^{0,\mathrm{TSO}}\tag{25}$$

$$\begin{aligned}&\mu_{PG^{\mathrm{DSO}i}}-\sigma_{PG^{\mathrm{DSO}i}}\leqslant\mu_{PD^{\mathrm{DSO}i}}\leqslant\mu_{PG^{\mathrm{DSO}i}}+\sigma_{PG^{\mathrm{DSO}i}},\\ &\quad\text{if }\mu_{PG^{\mathrm{DSO}i}}>0\&\sigma_{PG^{\mathrm{DSO}i}}>0\end{aligned}\tag{26}$$

$$\begin{aligned}&-\mu_{PG^{\mathrm{DSO}i}}-\sigma_{PG^{\mathrm{DSO}i}}\leqslant\mu_{PD^{\mathrm{DSO}i}}\leqslant-\mu_{PG^{\mathrm{DSO}i}}+\sigma_{PG^{\mathrm{DSO}i}},\\ &\quad\text{if }\mu_{PG^{\mathrm{DSO}i}}\leqslant 0\&\sigma_{PG^{\mathrm{DSO}i}}>0\end{aligned}\tag{27}$$

$$0\leqslant\sigma_{PD^{\mathrm{DSO}i}}\leqslant\sigma_{PG^{\mathrm{DSO}i}}\tag{28}$$

In the above equations, $P_{nt}^{0,\mathrm{TSO}}$, $P_{nt}^{s,\mathrm{TSO}}$ and $\Delta P_{nt}^{s,TSO}$ represent power generation in the base case, scenario case and their mismatch respectively for TSO. In equation (24), $P^{v,\mathrm{TSO}}=[P_{nt}^{0,\mathrm{TSO}},P_{nt}^{s,\mathrm{TSO}}]$.

2) DSO Formulation

$$\min\left\{\begin{array}{l}f_n^{v,\mathrm{DSO}i}\left(P^{v,\mathrm{DSO}i},\mu_{PG^{\mathrm{DSO}i}},\sigma_{PG^{\mathrm{DSO}i}}\right)+\\ \rho_{\mathrm{DSO}i}^k(\mu_{PG^{\mathrm{DSO}i}}-\mu_{PD^{\mathrm{DSO}i}})+\\ \left\|\eta_{\mathrm{DSO}i}^k\circ(\mu_{PG^{\mathrm{DSO}i}}-\mu_{PD^{\mathrm{DSO}i}})\right\|^2+\\ \alpha_{\mathrm{DSO}i}^k(\sigma_{PG^{\mathrm{DSO}i}}-\sigma_{PD^{\mathrm{DSO}i}})+\\ \left\|\beta_{\mathrm{DSO}i}^k\circ(\sigma_{PG^{\mathrm{DSO}i}}-\sigma_{PD^{\mathrm{DSO}i}})\right\|^2\end{array}\right\}\tag{29}$$

where

$$f_n^{v,\mathrm{DSO}i}\left(P^{v,\mathrm{DSO}i},\mu_{PD^{\mathrm{DSO}i}},\sigma_{PD^{\mathrm{DSO}i}}\right)=$$

$$\min \sum_t \sum_n \left\{ \begin{array}{l} \left\{ c_{nt}\left(P_{nt}^{0,\mathrm{DSO}i}\right) I_{nt}^{0,\mathrm{DSO}i} + SUD_{nt} \right\} + \\ \sum_{s=1}^{\mathrm{NS}} p_s \left\{ \sum_t \sum_n c_{nt}\left(\Delta P_{nt}^{s,\mathrm{DSO}i}\right) I_{nt}^{s,\mathrm{DSO}i} \right\} \end{array} \right\} \tag{30}$$

Subject to:

Constraints are given in (2A)–(3A), (4)–(6), (7A)–(8A), (9)–(11), (12A)–(13A), (14)

$$\Delta P_{nt}^{s,\mathrm{DSO}i} = P_{nt}^{s,\mathrm{DSO}i} - P_{nt}^{0,\mathrm{DSO}i} \tag{31}$$

$$\mu_{PD^{\mathrm{DSO}i}} - \sigma_{PD^{\mathrm{DSO}i}} \leqslant \mu_{PG^{\mathrm{DSO}i}} \leqslant \mu_{PD^{\mathrm{DSO}i}} + \sigma_{PD^{\mathrm{DSO}i}}, \quad \text{if } \mu_{PD^{\mathrm{DSO}i}} > 0 \,\&\, \sigma_{PD^{\mathrm{DSO}i}} > 0 \tag{32}$$

$$-\mu_{PD^{\mathrm{DSO}i}} - \sigma_{PD^{\mathrm{DSO}i}} \leqslant \mu_{PG^{\mathrm{DSO}i}} \leqslant -\mu_{PD^{\mathrm{DSO}i}} + \sigma_{PD^{\mathrm{DSO}i}}, \quad \text{if } \mu_{PD^{\mathrm{DSO}i}} \leqslant 0 \,\&\, \sigma_{PD^{\mathrm{DSO}i}} > 0 \tag{33}$$

$$0 \leqslant \sigma_{PG^{\mathrm{DSO}i}} \leqslant \sigma_{PD^{\mathrm{DSO}i}} \tag{34}$$

Here, $P_{nt}^{0,\mathrm{DSO}i}$, $P_{nt}^{s,\mathrm{DSO}i}$ and $\Delta P_{nt}^{s,\mathrm{DSO}i}$ represent the power generation in the base case, scenario case and their mismatch respectively for the ith DSO. As well, in equation (30) $P^{v,\mathrm{DSO}i} = [P_{nt}^{0,\mathrm{DSO}i}, P_{nt}^{s,\mathrm{DSO}i}]$.

B. Proposed Method II: Formulation of Mean and Standard Deviation Based Stochastic Coordination for Solving SSCUC with Quadratic Penalty

Proposed method II (PM-II) has utilized the quadratic penalty function to evaluate the SSCUC problem. The generalized equation presented in (19) can be rewritten as:

$$\begin{aligned} \min\ & f^v(X^v, Y) + w_\mu \circ (\mu_{T^v} - \mu_{R^v})^2 + w_\sigma \circ (\sigma_{T^v} - \sigma_{R^v})^2 \\ \text{s.t. } & P_r[g_m(X^v, Y) \leqslant 0] \geqslant \omega_m, \\ & m = 1, 2, 3, \ldots, M \\ & P_r[h_{m'}(X^v, Y) = 0] \geqslant \omega_{m'}, \\ & m = 1, 2, 3, \ldots, M' \end{aligned} \tag{35}$$

In this formulation, the mean and standard deviation of the boundary variables are utilized as shared variables. Furthermore, the mean and standard deviation of the non-separable function is utilized in the penalty function. In addition, the penalty function with a quadratic term is used instead of Lagrange penalty terms. Also, in equation (35), $\mu_{T^v} = \mu_{PG^{\mathrm{DSO}i}}$, $\mu_{R^v} = \mu_{PD^{\mathrm{DSO}i}}$, $\mu_{T^v} = \mu_{PG^{\mathrm{DSO}i}}$, $\mu_{R^v} = \mu_{PD^{\mathrm{DSO}i}}$ substitutions can be made for the TSO and DSO formulations in (36) and (41).

1) TSO Formulation

$$\min \left\{ \begin{array}{l} f_n^{v,\mathrm{TSO}}\left(P^{v,\mathrm{TSO}}, \mu_{PD^{\mathrm{DSO}i}}, \sigma_{PD^{\mathrm{DSO}i}}\right) + \\ \sum_{i=1}^{I} \{ w_\mu^{\mathrm{DSO}i,k} (\mu_{PD^{\mathrm{DSO}i}} - \mu_{PG^{\mathrm{DSO}i}})^2 + \\ w_\sigma^{\mathrm{DSO}i,k} (\sigma_{PD^{\mathrm{DSO}i}} - \sigma_{PG^{\mathrm{DSO}i}})^2 \} \end{array} \right\} \tag{36}$$

Subject to:

Constraints are given in (2)–(14)

$$\Delta P_{nt}^{s,\mathrm{TSO}} = P_{nt}^{s,\mathrm{TSO}} - P_{nt}^{0,\mathrm{TSO}} \tag{37}$$

$$\mu_{PG^{\mathrm{DSO}i}} - \sigma_{PG^{\mathrm{DSO}i}} \leqslant \mu_{PD^{\mathrm{DSO}i}} \leqslant \mu_{PG^{\mathrm{DSO}i}} + \sigma_{PG^{\mathrm{DSO}i}}, \quad \text{if } \mu_{PG^{\mathrm{DSO}i}} > 0 \,\&\, \sigma_{PG^{\mathrm{DSO}i}} > 0 \tag{38}$$

$$-\mu_{PG^{\mathrm{DSO}i}} - \sigma_{PG^{\mathrm{DSO}i}} \leqslant \mu_{PD^{\mathrm{DSO}i}} \leqslant -\mu_{PG^{\mathrm{DSO}i}} + \sigma_{PG^{\mathrm{DSO}i}}, \quad \text{if } \mu_{PG^{\mathrm{DSO}i}} \leqslant 0 \,\&\, \sigma_{PG^{\mathrm{DSO}i}} > 0 \tag{39}$$

$$0 \leqslant \sigma_{PD^{\mathrm{DSO}i}} \leqslant \sigma_{PG^{\mathrm{DSO}i}} \tag{40}$$

2) DSO Formulation

$$\min \left\{ \begin{array}{l} f_n^{v,\mathrm{DSO}i}\left(P^{v,\mathrm{DSO}i}, \mu_{PG^{\mathrm{DSO}i}}, \sigma_{PG^{\mathrm{DSO}i}}\right) + \\ w_\mu^{\mathrm{DSO}i,k} (\mu_{PG^{\mathrm{DSO}i}} - \mu_{PD^{\mathrm{DSO}i}})^2 + \\ w_\sigma^{\mathrm{DSO}i,k} (\sigma_{PG^{\mathrm{DSO}i}} - \sigma_{PD^{\mathrm{DSO}i}})^2 \end{array} \right\} \tag{41}$$

Subject to:

Constraints are given in (2A)–(3A), (4)–(6), (7A)–(8A), (9)–(11), (12A)–(13A), (14)

$$\Delta P_{nt}^{s,\mathrm{DSO}i} = P_{nt}^{s,\mathrm{DSO}i} - P_{nt}^{0,\mathrm{DSO}i} \tag{42}$$

$$\mu_{PD^{\mathrm{DSO}i}} - \sigma_{PD^{\mathrm{DSO}i}} \leqslant \mu_{PG^{\mathrm{DSO}i}} \leqslant \mu_{PD^{\mathrm{DSO}i}} + \sigma_{PD^{\mathrm{DSO}i}}, \quad \text{if } \mu_{PD^{\mathrm{DSO}i}} > 0 \,\&\, \sigma_{PD^{\mathrm{DSO}i}} > 0 \tag{43}$$

$$-\mu_{PD^{\mathrm{DSO}i}} - \sigma_{PD^{\mathrm{DSO}i}} \leqslant \mu_{PG^{\mathrm{DSO}i}} \leqslant -\mu_{PD^{\mathrm{DSO}i}} + \sigma_{PD^{\mathrm{DSO}i}}, \quad \text{if } \mu_{PD^{\mathrm{DSO}i}} \leqslant 0 \,\&\, \sigma_{PD^{\mathrm{DSO}i}} > 0 \tag{44}$$

$$0 \leqslant \sigma_{PG^{\mathrm{DSO}i}} \leqslant \sigma_{PD^{\mathrm{DSO}i}} \tag{45}$$

C. Solution Procedure

Figure 3 shows the flowchart of the proposed algorithm. Inner and outer loops are represented by red and green dashed line boxes. Following is the proposed algorithm flow for solving the SSCUC problem for coordinated TSDS:

1) Initially, multipliers are initialized and targets are assumed and provided to DSOs. DSOs will evaluate its SSCUC problem using (29) for PM-I and (41) for PM-II and $\mu_{PD^{\mathrm{DSO}i}}, \sigma_{PD^{\mathrm{DSO}i}}$ are evaluated for each DSO. Then, DSOs will send responses $\mu_{PD^{\mathrm{DSO}i}}, \sigma_{PD^{\mathrm{DSO}i}}$ to TSO.

2) TSO will receive responses from each DSO and solve its SSCUC problem for the evaluation of targets $\mu_{PG^{\mathrm{DSO}i}}, \sigma_{PG^{\mathrm{DSO}i}}$ using formulations in equation (23) for PM-I and (36) for PM-II.

3) The inner loop will consider the previous minimum cost of the outer loop and will try to achieve less cost than that for the new initial targets provided by the outer loop. An iterative inner loop will continue to evaluate targets and responses until the mismatch between targets and responses is below the threshold.

Consistency conditions:

$$|\mu_{PG^{\mathrm{DSO}i}} - \mu_{PD^{\mathrm{DSO}i}}| \leqslant \varepsilon_1 \tag{46}$$

$$|\sigma_{PG^{\mathrm{DSO}i}} - \sigma_{PD^{\mathrm{DSO}i}}| \leqslant \varepsilon_2 \tag{47}$$

4) An iterative outer loop will change the multipliers or weighting factors to further reduce the overall system cost. Moreover, the outer loop provides new targets based on previous targets, which has a minimum cost.

The outer loop will check the following stopping rules if they are satisfied:

Sufficient conditions:

$$\left| \frac{Sys_{\mathrm{cost}}^k - Sys_{\mathrm{cost}}^{k-1}}{Sys_{\mathrm{cost}}^k} \right| \leqslant \varepsilon_3 \tag{48}$$

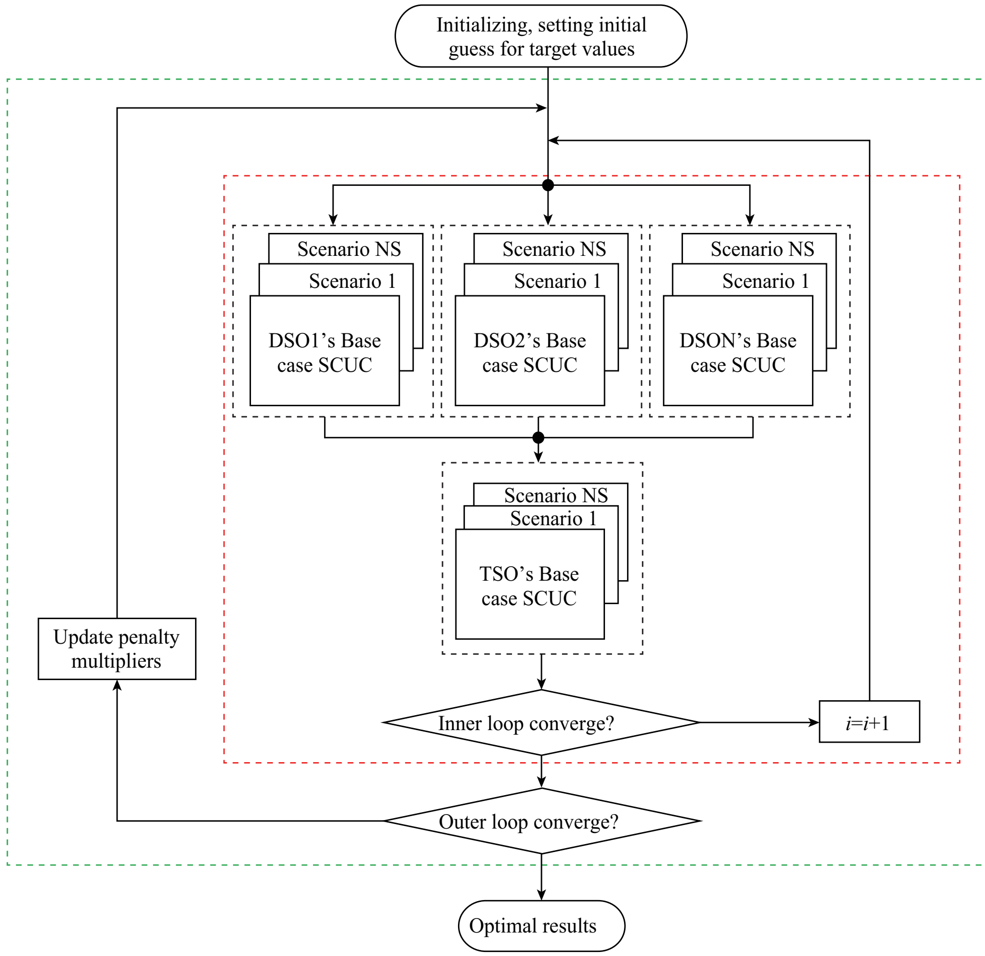

Fig. 3. PATC based stochastic TSDS coordination for solving SSCUC.

where

$$Sys_{\text{cost}}^{k} = TS_{\text{cost}}^{k} + \sum_{i=1}^{I} DS_{\text{cost}}^{i,k} \tag{49}$$

Updating multipliers: If the above conditions are satisfied, then end the iteration, otherwise update the multipliers by using the following formulas. For PM-I,

$$\rho_{\text{DSO}i}^{k+1} = \rho_{\text{DSO}i}^{k} - 2(\eta_{\text{DSO}i}^{k})^2 \times (\mu_{PG^{\text{DSO}i}} - \mu_{PD^{\text{DSO}i}}) \tag{50}$$

$$\eta_{\text{DSO}i}^{k+1} = \gamma_1 \eta_{\text{DSO}i}^{k} \tag{51}$$

$$\alpha_{\text{TSO}}^{k+1} = \alpha_{\text{TSO}}^{k} - 2(\beta_{\text{TSO}}^{k})^2 \times (\sigma_{PD^{\text{DSO}i}} - \sigma_{PG^{\text{DSO}i}}) \tag{52}$$

$$\beta_{\text{TSO}}^{k+1} = \gamma_2 \beta_{\text{TSO}}^{k} \tag{53}$$

For PM-II, weighing factor that should be updated are as follows:

$$w_{\mu}^{\text{DSO}i,k} = \gamma_3 w_{\mu}^{\text{DSO}i,k} \tag{54}$$

$$w_{\sigma}^{\text{DSO}i,k} = \gamma_4 w_{\sigma}^{\text{DSO}i,k} \tag{55}$$

5) The algorithm repeats the steps 2–6 until the stopping criteria is satisfied.

D. Discussion on Convergence of the Proposed Algorithm

In PATC, the deviation between the probabilistic system response and target should be iteratively reduced until it can be reduced no further provided that the system consistency is satisfied. So, the iterative process needs an appropriate coordination strategy to achieve convergence. In equation (56), $F_n^{v,k}$ is considered as an overall cost for decentralized coordination problem for the kth outer loop, which is the sum of the TSO and DSO problems.

$$\begin{aligned}&F_n^{v,k}\left(X_0^{\text{TSO},k}, X_0^{\text{DSO}i,k}, X_1^k, X_2^k, X_3^k, X_4^k\right) = \\ &\left\{\begin{aligned}&F_n^{v,\text{TSO},k}\Big(X_0^{\text{TSO},k}, X_1^k, X_2^k, \pi(X_1^k - X_3^k),\\ &\pi(X_2^k - X_4^k)\Big) + F_n^{v,\text{DSO}i,k}\Big(X_0^{\text{DSO}i,k}, X_3^k, X_4^k,\\ &\pi(X_3^k - X_1^k), \pi(X_4^k - X_2^k)\Big)\end{aligned}\right\}\end{aligned} \tag{56}$$

where $X_0^{\text{TSO},k} = P^{v,\text{TSO}}$, $X_1^k = \mu_{PD^{\text{DSO}i}}$, $X_2^k = \sigma_{PD^{\text{DSO}i}}$, $X_0^{\text{DSO}i,k} = P^{v,\text{DSO}i}$, $X_3^k = \mu_{PG^{\text{DSO}i}}$, $X_4^k = \sigma_{PG^{\text{DSO}i}}$, $F_n^{v,\text{TSO},k}$ is TSO cost, and $F_n^{v,\text{DSO}i,k}$ is DSO cost kth outer loop.

Here, equation (56) represents the non-convex optimization function, which deals with TSO and DSO coordination, as the convergence of the deterministic ATC has already been proved as a coordination strategy [27], even for non-convexity [25], [26]. Hence, the PATC process can follow the coordination strategy which is the same as ATC, and can achieve convergence.

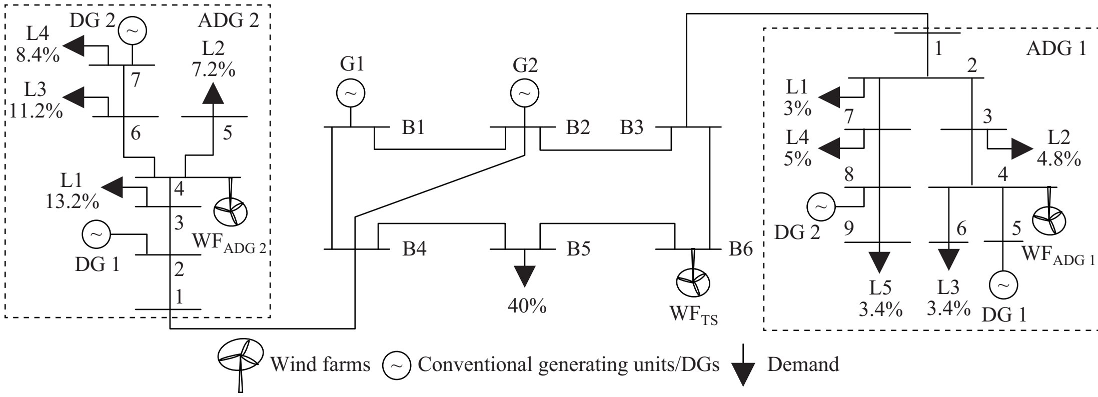

Fig. 4. Six-bus test system with wind farm at B6, connected to two active grids with wind farms at B3 and B4.

In the iterative process, the inner loop will reduce the cost of each system while following its shared variables and trying to reduce the deviation between targets and responses. Conversely, the outer loop will decrease the overall cost of the system (the sum of the costs of the TSO and DSOs). For $(k+1)$th outer loop, the overall system cost will be:

$$F_n^{v,k+1}\left(X_0^{\mathrm{TSO},k+1}, X_0^{\mathrm{DSO}i,k+1}, X_1^{k+1}, X_2^{k+1}, X_3^{k+1}, X_4^{k+1}\right) = \left\{ \begin{array}{l} F_n^{v,\mathrm{TSO},k+1}\Bigg(X_0^{\mathrm{TSO},k+1}, X_1^{k+1}, X_2^{k+1}, \\ \pi\left(X_1^{k+1} - X_3^{k+1}\right), \pi\left(X_2^{k+1} - X_4^{k+1}\right)\Bigg) + \\ F_n^{v,\mathrm{DSO}i,k+1}\Bigg(X_0^{\mathrm{DSO}i,k+1}, X_3^{k+1}, X_4^{k+1}, \\ \pi\left(X_3^{k+1} - X_1^{k+1}\right), \pi\left(X_4^{k+1} - X_2^{k+1}\right)\Bigg) \end{array} \right\} \tag{57}$$

Hence, equation (56) is converted to (57) by replacing k with $k+1$.

Furthermore, PATC can utilize the top-bottom strategy and bottom-up strategy. However, the bottom-up strategy has been proven for fast convergence when compared to the top-down strategy [21]. Thus, the proposed algorithm has been started at a lower level of hierarchy because uncertainty cannot be controlled at this level. In addition, this paper has utilized weighting factors and Lagrange multipliers for updating the process which can variably affect convergence speed [27]. It should be noted that PATC is using the Lagrange or quadratic penalty function, which will make sure the following equation will be satisfied:

$$F_n^{v,k+1}\left(X_0^{TSO,k+1}, X_0^{\mathrm{DSO}i,k+1}, X_1^{k+1}, X_2^{k+1}, X_3^{k+1}, X_4^{k+1}\right) \leqslant F_n^{v,k}\left(X_0^{TSO,k}, X_0^{\mathrm{DSO}i,k}, X_1^{k}, X_2^{k}, X_3^{k}, X_4^{k}\right) \tag{58}$$

Equation (58) leads to the convergence of the algorithm to a minimum cost. The deviations between X_1^k and X_2^k, X_3^k and X_4^k are reduced in every iteration of the inner loop. This would converge the solution at some intermediate stage where TS and DSs have adjusted their power inflow/outflow with less mismatch than the threshold. Additionally, equation (48) will converge the solution at minimum cost, where the cost deviation between the previous and current iteration is negligible. Then, the algorithm will converge at a point where there is less deviation between targets and responses than thresholds and less deviation in the cost of the previous and current iterations than the threshold.

TABLE I
DATA FOR GENERATION UNITS AND WIND FARMS IN TS, ADG1 AND ADG2

Area	Units	Bus Number	P_{min} (MW)	P_{max} (MW)	a (MBtu)	b (MBtu/ MWh)	c (MBtu/ MW^2h)
TS	G1	B1	40	220	0	40	0.01
	G2	B2	10	100	0	30	0.01
	WF_{TS}	B6	0	10	N/A	N/A	N/A
ADG1	DG1	5	5	15	140	5	0.04
	DG2	8	0	9	50	25	0.00
	WF_{AGD1}	4	0	25	N/A	N/A	N/A
ADG2	DG1	2	0	10	100	7	0.08
	DG2	7	0	10	65	3	0.03
	WF_{ADG2}	4	0	18	N/A	N/A	N/A

TABLE II
24-HOUR LOAD DATA AND COST PER HOUR FOR UNIT COMMITMENT

Hour	Pd (MW)	Cost ($)/hour	Hour	Pd (MW)	Cost ($)/hour
1	175	3360.6478	13	242	7599.2653
2	169	2937.1845	14	244	7824.7020
3	165	2754.6201	15	249	7744.3345
4	155	3563.4661	16	256	8628.0408
5	155	3820.3458	17	256	8439.1596
6	165	2433.0477	18	247	7938.5168
7	173	3000.8469	19	246	7906.7954
8	174	3215.8871	20	237	7443.8136
9	185	3833.4675	21	237	7118.0104
10	202	4834.7637	22	233	7234.9520
11	228	6972.0649	23	210	5937.4443
12	236	6891.0348	24	210	5833.3913

IV. RESULTS AND DISCUSSION

A. Experimental Setup

A test system utilized in [14], is used for the transmission and distribution system. However, it is modified further to involve wind farms at different locations in TS and DS. Moreover, another test system involves a modified IEEE 118 bus system as TS while ADGs in the previous case are considered as DSs. In addition, the simulation has been performed on a core i7 2.7 GHz with 8 GB RAM, having Matlab r2018a. Matpower has been used for OPF based SCUC analysis and for obtaining IEEE system datasets [28]. In the proposed algorithm, $\rho^k_{\text{DSO}i}, \alpha^k_{\text{DSO}i}, w^{\text{DSO}i,k}_{\mu}$ and $\eta^k_{\text{DSO}i}, \beta^k_{\text{DSO}i}, w^{\text{DSO}i,k}_{\sigma}$ are set as column vectors of 0 and 1 respectively, while $\gamma_1, \gamma_2, \gamma_3, \gamma_4$ are set as column vectors of 1.5 at the start of every hour for all case studies. Additionally, thresholds $\varepsilon_1, \varepsilon_2$, and ε_3 are set to 1e-4, 1e-4, and 1e-3.

TABLE III
RESULTS' COMPARISON FOR PM-I AND PM-II

Number of Scenarios	PM-I Total cost ($)	PM-I Execution time (s)	PM-II Total cost ($)	PM-II Execution time (s)
20	135119.1151	185.2190	135015.3821	309.4129
50	141636.8275	295.3073	141511.2441	418.7810
100	170243.8193	405.4512	170101.3706	621.3169
200	221157.7063	835.2105	221005.5271	985.3681

TABLE IV
RESULTS' COMPARISON FOR CENTRALIZED AND DECENTRALIZED METHODS

Number of Scenarios	Centralized Total cost ($)	Centralized Execution time (s)	Decentralized Total cost ($)	Decentralized Execution time (s)	Optimality Gap (%)
20	131649.41	13.7216	135119.11	185.2190	2.63
50	136691.73	30.6639	141636.82	295.3073	3.61
100	156198.63	65.3857	170243.81	405.4512	8.99
200	192407.39	123.7331	221157.70	835.2105	14.94

TABLE V
EXCHANGE OF POWER BETWEEN TS AND DSs FOR 20 SCENARIOS

Number of Scenarios	Net Power Flow TS-ADG1	Net Power Flow TS-ADG2	Number of Scenarios	Net Power Flow TS-ADG1	Net Power Flow TS-ADG2
0	−1.5483	19.8377	11	−1.2514	19.2802
1	−1.7261	19.8377	12	−1.8591	18.7592
2	−2.0255	20.9139	13	−1.0473	18.1000
3	−2.1540	20.1000	14	−2.0327	19.3442
4	−1.2136	20.9040	15	−1.0948	20.0440
5	−1.3134	21.0997	16	−1.6265	20.1000
6	−1.7259	20.5997	17	−2.4603	21.2465
7	−1.9030	19.5997	18	−1.5711	21.7551
8	−1.7935	19.5109	19	−1.8142	20.8377
9	−1.3710	19.1000	20	−1.3951	19.8377
10	−2.0155	19.8377			

Random hypercube sampling has been utilized for generating different scenarios of the system. Binomial distribution and Weibull distribution are utilized for generating random samples of generators and wind farms respectively. Single line diagrams and system data are provided in each case study. Furthermore, K-means has been utilized for clustering a huge amount of uncertainty data into a few numbers of samples because it has been widely utilized for this purpose [29].

B. Case Study

1) Case 1: Six-Bus System As TS and 9-Bus and 7-Bus Systems As DSs

In this case, the 6-bus system is utilized as a transmission system while 9-bus (ADG1) and 7-bus (ADG2) systems are utilized as distribution systems. Also, a wind farm is added at bus B6 in TS while one wind farm is also added at bus 4 of both 7-bus and 9-bus systems.

2) Case 2: 118 Bus TS and 7 and 9 Bus DS

In this case, the 118-bus system is utilized as a transmission system while 9-bus (ADG1) and 7-bus (ADG2) systems are utilized as distribution systems. In addition, 10 wind farms are added at different buses in TS while one wind farm is also added at bus 4 of both 7-bus and 9-bus systems. A modified test system with TS and ADG1 and ADG2 is shown in Fig. 7.

TABLE VI
DATA FOR GENERATION UNITS AND WIND FARMS IN TS, ADG1 AND ADG2

Area	Units	Bus Number	$P_{\min}$ (MW)	$P_{\max}$ (MW)	a (MBtu)	b (MBtu/MWh)	c (MBtu/MW^2 h)
TS	G1–54	Given in standard IEEE 118-bus data					
	$WF1_{TS}$, - $WF10_{TS}$	B5, B9, B30, B37, B38, B63, B64, B68, B71, B81	0	10	N/A	N/A	N/A
ADG1	DG1	5	5	15	0	20	0.01
	DG2	8	0	9	0	25	0.01
	WF_{AGD1}	4	0	25	N/A	N/A	N/A
ADG2	DG1	2	0	10	0	20	0.01
	DG2	7	0	10	0	25	0.01
	WF_{ADG2}	4	0	18	N/A	N/A	N/A

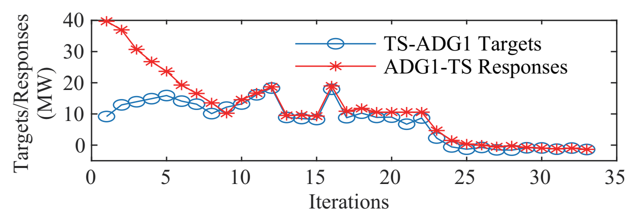

Fig. 5. Mismatch reduction between targets and responses of TS and ADG1.

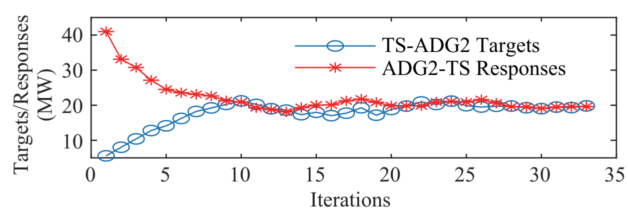

Fig. 6. Mismatch reduction between targets and responses of TS and ADG2.

C. Tests for Comparison of the Distribution of Targets and Responses

To show the efficacy of the results, we have performed a 1-sample t-test and a 2-sample t-test for comparing means and standard deviations obtained as targets and responses from TSO and DSOs respectively. Table X shows the results.

D. Comparison with Previous Research

Previous researchers have considered each scenario in the TSDS coordination problem as a separate coordination problem [19]. Then, the execution time will drastically increase with an increase in the number of scenarios. Table XI shows the comparison of the results of PM-I with the method presented in [19].

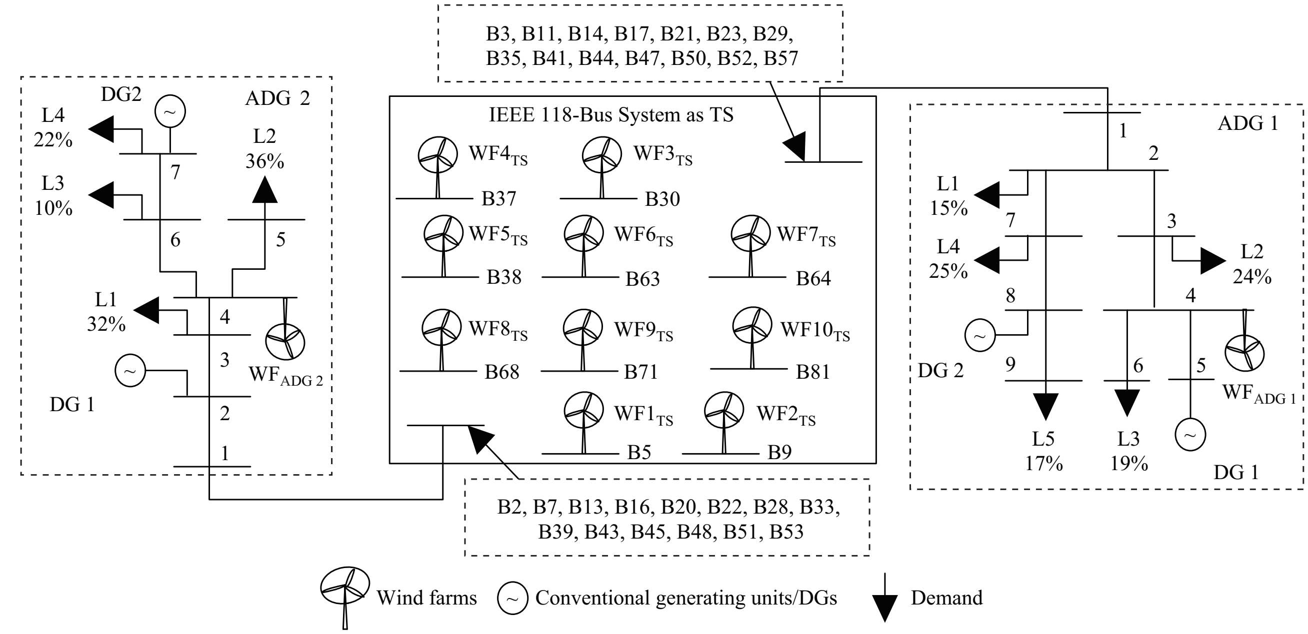

Fig. 7. Modified IEEE 118 bus system with multiple wind farms, connected to multiple active grids.

TABLE VII
24 HOUR LOAD DATA FOR UNIT COMMITMENT

Hour	Pd (MW)	Hour	Pd (MW)	Hour	Pd (MW)
1	4242	10	4731	17	4615
2	4331	11	4776	18	4565
3	4395	12	4809	19	4534
4	4487	13	4843	20	4472
5	4560	13	4784	21	4235
6	4580	14	4742	22	4205
7	4645	15	4702	23	4192
8	4689	16	4652	24	4212

TABLE VIII
RESULTS' COMPARISON FOR PM-I AND PM-II

Number of Scenarios	PM-I		PM-II	
	Total cost (million)	Execution time (s)	Total cost (million)	Execution time (s)
20	4.6514	674.7931	4.6512	791.8203
50	4.9155	911.5734	4.9147	1109.4193
100	5.2102	1257.7369	5.2091	1585.4930
200	5.6155	1518.8891	5.6139	1896.1106

TABLE IX
RESULTS' COMPARISON FOR CENTRALIZED AND DECENTRALIZED METHODS

Number of Scenarios	Centralized		Decentralized		Optimality Gap (%)
	Total cost (million)	Execution time (s)	Total cost (million)	Execution time (s)	
20	4.5029	5.5013	4.6514	674.7931	3.29
50	4.6428	17.9260	4.9155	911.5734	5.87
100	4.8609	54.3852	5.2102	1257.7369	7.18
200	5.0128	161.6148	5.6155	1518.8891	12.02

TABLE X
EVALUATION OF T-TEST AND T-TEST2 FOR TARGETS AND RESPONSES

Number of Scenarios	PM-I	PM-II
1-sample t-test	0	0
2-sample t-test	0	0

TABLE XI
RESULTS' COMPARISON OF PM-I AND METHOD PRESENTED IN [19]

Number of Scenarios	PM-I		Method [19]	
	Total cost	Execution time	Total Cost	Execution time
20	135119.1151	185.2190	138601.3109	333.4980
50	141636.8275	295.3073	146557.1331	445.8731
100	170243.8193	405.4512	171617.0271	624.1811
200	221157.7063	835.2105	247137.3149	1036.5002

V. CONCLUSION AND FUTURE DIRECTION

This paper has proposed the stochastic coordination algorithm for solving the coupled TS and DS SSCUC problem. This paper has presented two different penalty function based methods, which have utilized the mean and standard deviation of the shared variables instead of solving the coordination problem for each scenario. Therefore, this new approach has reduced the computational time and resources required to solve the probabilistic coordination problem. Moreover, the augmented Lagrange penalty function based proposed method (PM-I) has shown better convergence speed and minimization in large-scale systems than the quadratic penalty function based proposed method (PM-II).

The proposed methods can be applied to modern power system coordination with high penetration of renewable energy. To solve the stochastic coordination problem, PM-I and PM-II require less effort than current approaches dealing with each scenario as a separate coordination problem. In the future, more characteristics of shared variables' distribution can be studied to find better results while utilizing less computational resources.

REFERENCES

[1] P. De Martini, "Operational coordination architecture: new models and approaches," *IEEE Power and Energy Magazine*, vol. 17, no. 5, pp. 29–39, Sept. /Oct. 2019.

[2] Entso E. (2015). Towards Smarter Grids: Developing TSO and DSO Roles and Interactions for the Benefit of Consumers, [Online]. Availabe: https://eepublicdownloads. entsoe. eu/clean-documents/Publications/Position%20papers%20and%20reports/150303_ENTSO-E_Position_Paper_TSO-DSO_interaction. pdf.

[3] Entso E. General guidelines for reinforcing the cooperation between TSOs and DSOs[Online]. Available: https://eepublicdownloads. entsoe. eu/clean-documents/Publications/Position%20papers%20and%20 reports/entsoe_pp_TSO-DSO_web. pdf.

[4] (2014). Olivine Report on Distributed Energy Resources Integration: Summarizing the Challenges and Barriers [Online]. Available: http://www. caiso. com/Documents/OlivineReport_DistributedEnergy ResourceChallenges_Barriers. pdf.

[5] A. Olson, A. Mahone, E. Hart, J. Hargreaves, R. Jones, N. Schlag, G. Kwok, N. Ryan, R. Orans, and R. Frowd, "Halfway there: can california achieve a 50% renewable grid?," *IEEE Power and Energy Magazine*, vol. 13, no. 4, pp. 41–52, Jul. /Aug. 2015.

[6] FERC and NAERC, "Arizona-southern california outages on September 8, 2011: causes and recommendations," *FERC and NERC*, 2012.

[7] J. Kabouris and F. D. Kanellos, "Impacts of large-scale wind penetration on designing and operation of electric power systems," *IEEE Transactions on Sustainable Energy*, vol. 1, no. 2, pp. 107–114, Jul. 2010.

[8] Y. Wang, S. Q. Zhao, Z. Zhou, A. Botterud, Y. Xu, and R. Z. Chen, "Risk adjustable day-ahead unit commitment with wind power based on chance constrained goal programming," *IEEE Transactions on Sustainable Energy*, vol. 8, no. 2, pp. 530–541, Apr. 2017.

[9] D. Bertsimas, E. Litvinov, X. A. Sun, J. Y. Zhao, and T. X. Zheng, "Adaptive robust optimization for the security constrained unit commitment problem," *IEEE Transactions on Power Systems*, vol. 28, no. 1, pp. 52–63, Feb. 2013.

[10] A. Papavasiliou, S. S. Oren, and R. P. O'Neill, "Reserve requirements for wind power integration: a scenario-based stochastic programming framework," *IEEE Transactions on Power Systems*, vol. 26, no. 4, pp. 2197–2206, Nov. 2011.

[11] Z. S. Li, Q. L. Guo, H. B. Sun, and J. H. Wang, "Coordinated economic dispatch of coupled transmission and distribution systems using heterogeneous decomposition," *IEEE Transactions on Power Systems*, vol. 31, no. 6, pp. 4817–4830, Nov. 2016.

[12] Z. S. Li, Q. L. Guo, H. B. Sun, and J. H. Wang, "Coordinated transmission and distribution AC optimal power flow," in *2017 IEEE Power & Energy Society General Meeting*, 2017.

[13] A. Nawaz and H. Wang, "Risk-Aware Distributed Optimal Power Flow in Coordinated Transmission and Distribution System, " in *Journal of Modern Power Systems and Clean Energy* (Early Access), doi: 10.35833/MPCE.2019.000005

[14] A. Kargarian and Y. Fu, "System of systems based security-constrained unit commitment incorporating active distribution grids," *IEEE Transactions on Power Systems*, vol. 29, no. 5, pp. 2489–2498, Sep. 2014.

[15] A. Nawaz, H. T. Wang, Q. W. Wu, and M. K. Ochani, "TSO and DSO with large-scale distributed energy resources: A security constrained unit commitment coordinated solution," *International Transactions on Electrical Energy Systems*, vol. 30, no. 3, pp. e12233, Mar. 2020.

[16] X. Liu, Y. Liu, J. Liu, Y. Xiang and X. Yuan, "Optimal planning of AC-DC hybrid transmission and distributed energy resource system: Review and prospects, " in *CSEE Journal of Power and Energy Systems*, vol. 5, no. 3, pp. 409-422, Sept. 2019

[17] J. Yu, Y. Guo and H. Sun, "Testbeds for integrated transmission and distribution networks: Generation methodology and benchmarks, " in *CSEE Journal of Power and Energy Systems*, vol. 6, no. 3, pp. 518-527, Sept. 2020

[18] C. H. Wang and Y. Fu, "Fully parallel stochastic security-constrained unit commitment," *IEEE Transactions on Power Systems*, vol. 31, no. 5, pp. 3561–3571, Sep. 2015.

[19] M. Khanabadi, Y. Fu, and L. Gong, "A fully parallel stochastic multiarea power system operation considering large-scale wind power integration," *IEEE Transactions on Sustainable Energy*, vol. 9, no. 1, pp. 138–147, Jan. 2017.

[20] F. X. Wang, M. Xiao, and L. Gao, "Probabilistic analytical target cascading combined with Kriging metamodel for multidisciplinary robust design optimization," in *2015 IEEE International Conference on Industrial Engineering and Engineering Management (Ieem)*, 2015, pp. 1407–1411.

[21] H. B. Liu, W. Chen, M. Kokkolaras, P. Y. Papalambros, and H. M. Kim, "Probabilistic analytical target cascading: a moment matching formulation for multilevel optimization under uncertainty," *Journal of Mechanical Design*, vol. 128, no. 4, pp. 991–1000, Jul. 2006.

[22] Y. Fu, Z. Y. Li, and L. Wu, "Modeling and solution of the large-scale security-constrained unit commitment," *IEEE Transactions on Power Systems*, vol. 28, no. 4, pp. 3524–3533, Nov. 2013.

[23] C. H. Wang and Y. Fu, "A distributed calculation of global shift factor considering information privacy," *IEEE Transactions on Power Systems*, vol. 31, no. 5, pp. 4161–4162, Sep. 2016.

[24] H. M. Kim, M. Kokkolaras, L. S. Louca, G. J. Delagrammatikas, N. F. Michelena, Z. S. Filipi, P. Y. Papalambros, J. L. Stein, D. N. Assanis, "Target cascading in vehicle redesign: a class VI truck study," *International Journal of Vehicle Design*, vol. 29, no. 3, pp. 199–225, Jan. 2002.

[25] H. M. Kim, W. Chen, and M. M. Wiecek, "Lagrangian coordination for enhancing the convergence of analytical target cascading," *AIAA Journal*, vol. 44, no. 10, pp. 2197–2207, Oct. 2006.

[26] S. DorMohammadi and M. Rais-Rohani, "Exponential penalty function formulation for multilevel optimization using the analytical target cascading framework," *Structural and Multidisciplinary Optimization*, vol. 47, no. 4, pp. 599–612, Apr. 2013.

[27] J. J. Michalek and P. Y. Papalambros, "Weights, norms, and notation in analytical target cascading," *Journal of Mechanical Design*, vol. 127, no. 3, pp. 499–501, May 2005.

[28] R. D. Zimmerman, C. E. Murillo-Sánchez, and R. J. Thomas, "MATPOWER: steady-state operations, planning, and analysis tools for power systems research and education," *IEEE Transactions on Power Systems*, vol. 26, no. 1, pp. 12–19, Feb. 2011.

[29] L. Baringo and A. J. Conejo, "Correlated wind-power production and electric load scenarios for investment decisions," *Applied Energy*, vol. 101, pp. 475–482, Jan. 2013.

Aamir Nawaz received the B.Sc. (2009) and M.Sc. (2014) degrees in Electrical Engineering from Pakistan. He is currently pursuing his Ph.D. degree in Electrical Engineering at Shandong University, Jinan, China. He has three years of industrial experience and eight years of teaching experience. His research interests include power system optimization, economics, planning, and integration of high scale renewable energy.

Hongtao Wang (M'04–SM'15) received the B.Sc. and M.Sc. degrees in Electrical Engineering from Shandong Polytechnic University, Jinan, China, in 1995 and 1998, respectively, and his Ph.D. degree in Electrical Engineering from Shandong University, Jinan, in 2005.

He was a Postdoctoral Researcher with the Department of Computer Science, Shandong University. From 2005 to 2010, he was an Associate Professor with the School of Electrical Engineering, Shandong University, where he has been a Professor since 2010. His research interests include power system analysis, control, and smart grids.